

DUAL SCATTERING CHANNEL SCHEMES EXTENDING THE JOHNS ALGORITHM

STEFFEN HEIN

ABSTRACT. Dual scattering channel schemes extend the transmission line matrix numerical method (JOHNS' TLM algorithm) in two directions. For one point, transmission line links are replaced by abstract scattering channels in terms of paired distributions (characteristic impedances are thus neither needed, nor in general defined, e.g.). In the second place, non-trivial cell interface scattering is admitted during the connection cycle. Both extensions open a wide field of applications beyond the range of classical time domain schemes, such as YEE's FDTD method and TLM.

A DSC heat propagation [diffusion] scheme in non-orthogonal mesh, wherein heat sources are coupled to a lossy Maxwell field, illustrates the approach.

Westerham on February 8, 2020

1. INTRODUCTION

It seems a paradox - and is just a typical process in mathematical analysis that a structure turns simple in a more general setting which at the same time enlarges its range of application. Accordingly - not very surprising - some ill-famed 'intricacies of the propagator approach to TLM' (sic. Rebel [1], p. 5) virtually vanish if some of its elements are taken as the building blocks of a more general scheme. In fact, constructing the latter on essentially these elements in a quasi axiomatic manner will prove such intricacies to be mere artefacts of an inadequate framework.

The choice of elements proposed in this paper 'generalizes' the Johns algorithm in two directions. In the first place, abstract scattering channels replace transmission lines, which have some unpleasant properties (section 2). Secondly, non-trivial cell boundary (*interface*) scattering is permitted during the connection cycle. The schemes thus obtained are characterized by a non-trivial two-step (*connection-reflection*) cycle of iteration which exhibits certain duality relations - whence their name.

When P.B. Johns and co-workers introduced the transmission line matrix (TLM) numerical method in the 1970s [2] it was almost instantaneously assimilated by the microwave engineering community. In the same audience the method remained until today subject of assiduous study and extensive publication. Three conferences explicitly focussed on TLM [3, 4, 5], and the monographs of Christopoulos [6] and Cogan [7] deal in detail with the original ideas as well as with classical applications.

Key words and phrases. Time domain methods, TLM, FDTD, Green's function techniques, hyperbolic PDE.

A familiarity with the transmission line picture, and the well known scattering concept, certainly fostered the acceptance of the TLM method among microwave engineers. On the other hand, just so the primary interest turned of course on applications in their own discipline, rather than onto the inner algorithmic structure as an object of mathematical analysis. Over the years still a node more was routinely invented, with new dispersion characteristics and/or equipped with still another ingenious stub, designed to model special propagation or transport phenomena, in varied geometries or boundary conditions. [8] stands somewhat exemplary for this line of research.

Mathematical questions, regarding the inner structure of the TLM algorithm and its potential generalizations, have thus apparently been for a long time of secondary interest. They have yet not been left completely out of view. Chen, Ney and Hoefer [9] proved equivalence of the original (expanded) TLM node without stubs [2, 10] to the Yee finite-difference grid [11, 12]. Recently, the non-trivial question of consistence of Johns' symmetrical condensed node (SCN), cf. Johns [13], with Maxwell's equations and the intimately related problem of convergence to a smooth solution for decreasing time step and grid spacing have been tackled, and in parts solved, by Rebel [1]. His thesis presents, by the way, a thorough survey over the ramifications of TLM until that time (year 2000), without perhaps spending sufficient attention to its non-orthogonal mesh extensions.

From a quite general viewpoint, viz. widely independent of any particular physical interpretation, the structure of the stub loaded (deflected) non-orthogonal TLM algorithm has been analysed in [14]. The present paper goes even further and challenges the transmission line picture at all. The latter, in universally imposing free wave propagation between cells (with great benefit, at times), induces modeling limitations under circumstances that are touched in section 2. Many restrictions can be by-passed by replacing transmission lines with abstract scattering channels in terms of 'paired' distributions.

Dual scattering channel schemes are characterized by a two-step updating cycle with certain duality relations between the two steps. The TLM method with its familiar connection-reflection cycle is trivial *as a dual scheme* in that the connection map reduces essentially to identity (viz. pure transmission or total reflection) - anew with modeling limitations. These are raised, again, in admitting non trivial cell interface scattering on the connection step of iteration.

One major merit of scattering channel schemes is unconditional stability under quite general circumstances. This is mainly due to a Green's function updating scheme (section 3) that as Johns' cycle is well known from the TLM method, and which provides clear cut and reliable stability criteria in the linear case (TLM, for instance). It is not entirely in the wrong to say that much of the substance of this paper consists in a straightforward derivation of discrete Green's function integrals (in the form of the connection and reflection maps defined in section 3) from a set of dynamical model equations (section 4). In fact, prepared by suitable definitions, the proceeding remains not far from trivial, and can be condensed in some simple

propositions (Theorem 1 and corollaries). At any rate, nothing obscure nor 'intricate' should so be associated anymore with the propagator approach.

DSC schemes open a new field of exploration far beyond the traditional time domain methods, FDTD and TLM. From the view-point of this study the classical TLM method appears as an especially simple (first order linear, trivially dual) DSC scheme, cf. section 4 - which, of course, does not contest by any means its *raison d'être* in its proper domain of application.

2. SCATTERING CHANNELS

Any extension of the TLM method that includes heat transfer, fluid flow, or particle current, for instance, involves scattering channels other than transmission lines. The latter, for a non vanishing real part of the characteristic line impedance, inherently impose wave propagation between cells. Degenerate lines, with a purely imaginary impedance, still work in diffusion models, cf. [6], chap.7. Other types of transport, or modes of propagation, such as for example the relativistic charged particle current treated in [14], are very unnaturally and more or less imperfectly modeled using transmission lines. There is good reason to get rid of lines in such and other cases, within an extended framework.

A first step towards the definition of more general scattering channels in TLM has been undertaken in replacing transmission lines with abstract projections into in- and outgoing field components, cf. [14]. It was postulated in this paper that the propagating fields ('link quantities') admit a decomposition into a direct sum

$$(1) \quad z = z_{in} \oplus z_{out} \quad ,$$

z_{in} and z_{out} representing the incident and outgoing fields, respectively. Moreover, it is essential in our understanding of TLM that the latter have a merely operational meaning in that only the total field z enters the dynamical model equations (cf. sections 3,4). In singular cases, a physical interpretation can yet still be given to z_{in} , z_{out} , on the basis of a special analysis, cf. [16], Corollary 2.

For the Maxwell field model, the technical passage from the transmission line formulation to the projection operator setting is outlined in [14], Appendix A

In the classical TLM setup the connection map simply transfers, without further modifications, the quantities outgoing from a port into quantities incident at an adjacent port of a neighbouring mesh cell, or also back into the same port if the latter is located at a totally reflecting wall. This is in perfect harmony with the behaviour of a propagating electromagnetic field, the components of which are tangential to the cell boundary (as the link quantities always are in a classical TLM cell, cf. [19]) and that is thus not subject to refractive scattering at the cell face, even if the medium changes there.

The situation is clearly not thus simple for arbitrary propagating quantities. To circumvent any modeling restrictions, the connection cycle of a non-trivial DSC scheme comprises cell interface scattering from the out-set. Nodal and cell face scattering thus enter into a kind of duality relation

that becomes visible, for instance, in an apparent symmetry of the model equations in their most general form (21, 25, 26). Nodal and cell boundary scattering may thus be of equal importance and sometimes boundary scattering plays even the leading rôle in a DSC algorithm.

In the generalized setup, just as in the traditional TLM framework, scattering channels interconnect a *node*, viz. a suitably defined *centre* of a mesh cell, with *ports* at the cell boundary. The channels are yet no longer represented by transmission lines. With respect to a computed physical field in D -dimensional configuration space, they form merely a pair of scalar or vector valued distributions, transposed over a distance in space, which test the field within the cell and on its boundary. A DSC scattering channel will be defined, precisely, as a pair of continuous linear functions (p, p^\sim) which act on a class of (suitably smooth real or complex) vector fields Z in configuration space, such that p has its support on a cell face and p^\sim is connected to p via pull back into the node, i.e.: Given any notion of *centre* of cell and face, as well as the spatial translation $s : \mathbb{R}^D \rightarrow \mathbb{R}^D$ that shifts the centre of a cell (*node*) into the centre of the face where p has its support, then the *nodal image* p^\sim of p is defined as the distribution

$$(2) \quad (p^\sim, Z) := (p \circ s, Z) = (p, Z \circ s^{-1}),$$

and the pair (p, p^\sim) is called a *scattering channel*. Equivalently, a scattering channel can of course be identified with (p, s) or even simply with the *port* p , the pertinent shift and nodal image then being tacitly understood. The concept should in fact not be handled in too rigid a fashion - and there is no need to do so. In certain applications the support of the port distribution may be extended over a neighbourhood of a face, or the node distribution be thought of rather a mean over the entire cell (in the way familiar from finite volume methods).

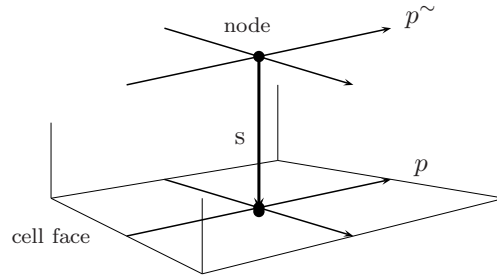


FIGURE 1. Ports on a cell face with their nodal images.

Needless to say that the stressed duality between nodal and cell boundary scattering is not to be misunderstood in the narrow sense of category theory. Here, it refers simply to the observation that a set of propositions are valid, modulo symmetry in certain terms, in the two scattering situations - which of course reflects the paired distribution concept of scattering channel and the already mentioned symmetry of the pertinent model equations in their most

general form. A parallel symmetry then clearly characterizes the structure of the reflection and connection maps that solve these equations.

Cell boundary scattering is, by the way, not thus new an option: Already in the TLM model for superconducting boundary [18] cell face s-parameters and boundary stubs have been introduced for solving the discretized London equations, cf. also [16].

Despite the abolition of transmission lines, in virtue of their replacement by abstract scattering channels the computed ('physical') fields can still be represented, in the way familiar from the classical TLM method, as sums of *in-* and *outgoing* scalar or vector fields

$$(3) \quad z = z_{in} + z_{out} \quad .$$

No physical interpretation or propagation property is, however, in general ascribed to $z_{in,out}$. In fact, these quantities are merely operationally defined by means of the well known Johns cycle

$$(4) \quad \begin{array}{ccc} z_{in} & = & (\mathcal{C}[z_{out}] + e) \quad \longleftarrow \\ z^p & = & z_{in} + z_{out} \quad \uparrow \\ \downarrow t + \tau/2 & & t + \tau \\ z_{out} & = & \mathcal{R}[z_{in}] \quad \uparrow \\ z^n & = & z_{in} + z_{out} \quad \longrightarrow \end{array} .$$

\mathcal{R} and \mathcal{C} denote the node and cell face propagators (or so-called reflection and connection maps - the latter including now cell boundary scattering, and $e = e(t)$ induces any excitation. Note again that z_{in}, z_{out} are so far *purely operational* quantities, i.e. only the total fields z enter the model equations, while z_{in}, z_{out} are *in general* bare of any physical meaning (a physical interpretation in terms of an energy flow still exists within the classical Maxwell field TLM model, cf. [16], Corollary 2).

As will be seen in the next section, the structures of the propagators \mathcal{R} and \mathcal{C} are very similar in the general DSC scheme, thus reflecting the dual rôle that nodal and boundary scattering play therein. In a sense, precised in section 3, \mathcal{R} and \mathcal{C} are the discrete *Green's function* (or *propagator*) *integrals* that in every Johns cycle strictly solve the model equations. In fact, the Johns cycle can be looked at as basically a two-step Green's function method for solving certain types of explicit finite difference equations in time.

Note that the model equations can in principle be directly solved inasmuch as they provide complete recurrence relations, cf. sections 3, 4. The Green's function approach (using Johns' cycle) offers, however, important advantages. Thus, it provides clear cut reliable stability criteria that make the DSC algorithm unconditionally stable under very general circumstances.

3. THE ELEMENTS CHARACTERIZING DSC SCHEMES

So far, we dealt on a more or less informal level with some typical traits of the TLM algorithm that either characterize DSC schemes in like manner, or which have to be modified in a specified way in order to attain a greater generality. We are, however, still bound to keep our introductory promise and give a coherent description of DSC schemes in terms of some quasi axioms

that condense their distinctive properties. Of course, we shall not really pursue axiomatics, here, in the sense of building a new theory on a complete set of first principles. (Nor are we adopting a dogmatic attitude and going to fix a rigid framework that, at times, should certainly be modified in one or another aspect, in order to better face a particular problem.) The emphasis is rather on compiling on a preliminary basis some formal elements that, in essence, lead to the peculiar structure of DSC schemes (in general), and of the TLM method (in particular), without being distracted by unnecessary information, such as mesh topology and geometry, s-parameters, e.g., which characterize only a singular physical interpretation.

In the following, '*simple*' definitions are visualized in writing the defined object(s) in *italics*, more crucial ones are explicitly designated as DEFINITIONS.

Until further notice, a *mesh* denotes only a non-void finite family (i.e. an indexed set) of elements named *cells*, which are sets in their turn, and share the following properties. Each cell ζ contains an element n_ζ , called its *node*, and a finite family $\partial\zeta = \{\partial\zeta_\iota\}$, called the (cell) *boundary*. The latter is built up of elements $\partial\zeta_\iota$, named *faces*, which are sometimes simply written ι in the place of $\partial\zeta_\iota$.

Definition 1. A mesh M is called *regular*, if and only if it satisfies the following requirements of *simplicity* (S) and *connectedness* (C):

- (S) Every node belongs to exactly one cell and every face to at most two cells in M .
- (C) For every two cells $\zeta^i, \zeta^j \in M$, there exists a connecting sequence $s = (\zeta^\kappa)_{\kappa=0}^k \in M^{\mathbb{N}}$, such that $\zeta^0 = \zeta^i, \zeta^k = \zeta^j$ and every two subsequent cells $\zeta^\kappa, \zeta^{\kappa+1}$ in s have a common face, for $0 \leq \kappa < k$.

Also - certainly not too misleading: Any two cells with a common face are called *adjacent* or *neighbouring* cells, and the common face a *connecting face* or *interface*.

By a first postulate, *DSC meshes are always regular meshes*.

The *state space* is any product of real or complex linear spaces labelled by the mesh cells

$$(5) \quad \mathcal{S} = \prod_{\zeta \in M} \mathcal{S}_\zeta \quad .$$

In addition, we require that a DSC state space always contains a non-void subspace $\mathcal{P} \subset \mathcal{S}$, named the space of *propagating fields*, which on every \mathcal{S}_ζ reduces to a product of 'squared' spaces in the following precise sense

$$(6) \quad \mathcal{P}_\zeta = \mathcal{P} \cap \mathcal{S}_\zeta = \prod_{\iota \in \partial\zeta} P_{\iota, \zeta}^2 \quad .$$

In a less formal language: Every propagating field z splits over the cells into a sequence of pairs

$$(7) \quad z_\zeta = (z_\iota, \tilde{z}_\iota)_{\iota \in \partial\zeta}$$

labelled by the faces of the cell boundary. It directly follows that there exists a canonical automorphism of \mathcal{P} which on every \mathcal{P}_ζ reduces to

$$(8) \quad \begin{aligned} nb & : \mathcal{P}_\zeta & \longrightarrow & \mathcal{P}_\zeta \\ (z_\iota, \tilde{z}_\iota) & \longmapsto & (\tilde{z}_\iota, z_\iota) & . \end{aligned}$$

nb is obviously involutory ($nb^2 = Id$), and is called the *node-boundary map*.

The components z_ι and z_ι^\sim in (7), (8) are named the *port* (or *face*-) *component*, and the *node component*, respectively, of $z = (z_\iota, z_\iota^\sim)$. They are usually written $z^p = z_\iota = \pi^p(z)$ and $z^n = z_\iota^\sim = \pi^n(z)$ with projections π^p, π^n that are canonically extended over the entire space \mathcal{P} .

Let $J := \bigcup_{\zeta \in M} \partial\zeta$ be the set of all faces in M (remember that $\partial\zeta$ has been introduced as a union of faces). Then, in virtue of (6), \mathcal{P} splits completely into subspaces

$$(9) \quad \mathcal{P} = \prod_{\iota \in J} \mathcal{P}_\iota \quad \text{with} \quad \mathcal{P}_\iota := \prod_{\zeta; \iota \in \partial\zeta} P_{\iota, \zeta}^2 \quad .$$

A *DSC process* is a step function of time

$$(10) \quad pr : [0, T) \longrightarrow \mathcal{S} \quad ,$$

such that $\pi^p \circ pr(t)$ and $\pi^n \circ pr(t - \tau/2)$ are constant on every time interval $[\mu\tau, (\mu+1)\tau)$, $\mu \in \mathbb{N}$, where they are defined. In other words:

Notation. Port components of a DSC process switch at integer multiples of the time step τ while node quantities switch at odd integer multiples of $\tau/2$.

Given a process, a state z with its entire history up to time t is usually written as a 'back in time running' sequence

$$(11) \quad [z](t) := (z(t - \mu\tau))_{\mu \in \mathbb{N}} \quad ,$$

expanding the domain of definition eventually to the negative time axis in the trivial way, i.e. $z(s) := 0$ for $s < 0$.

By this convention, we assign hence to index μ the (varying) state back in the past from present time t

$$(12) \quad [z]_\mu(t) := z(t - \mu\tau) \quad ,$$

rather than the (fixed) state $z(\mu\tau)$ - which has the technical advantage that μ so is directly related to a *time difference* (and eventually to an order of a finite difference equation in time), rather than to an *absolute time* (that is quite uninteresting, in general).

Functions defined on back in time running sequences, such as (10), are called *causal functions* (or *propagators*). Any such map is a discrete analogue to a causal Green's function (or 'propagator' -) integral, as for instance outlined in [16].

Let $X_0^\mathbb{N}$ denote the set of all sequences with an arbitrary, but finite, number of non-vanishing elements in a linear space X . For every mesh cell ζ and face ι in M , consider then the following subspaces of propagating fields $\mathcal{P}_\zeta^n := \pi^n(\mathcal{P}_\zeta)$, $\mathcal{P}_\iota^p := \pi^p(\mathcal{P}_\iota)$.

Definition 2. A *reflection map* (in $\zeta \in M$) is a (possibly time dependent) causal operator

$$(13) \quad \begin{aligned} \mathcal{R}_\zeta : (\mathcal{P}_\zeta^n)_0^\mathbb{N} &\longrightarrow \mathcal{P}_\zeta^n \\ [z^n] &\longmapsto \mathcal{R}_\zeta[z^n] \quad . \end{aligned}$$

Furthermore, a *connection map* (in $\iota \in J$) is a (possibly anew time dependent) causal operator

$$(14) \quad \begin{aligned} \mathcal{C}_\iota &: (\mathcal{P}_\iota^p)_0^\mathbb{N} \longrightarrow \mathcal{P}_\iota^p \\ [z^p] &\longmapsto \mathcal{C}_\iota[z^p] . \end{aligned}$$

Also, a *DSC system over M* is a pair $(\mathcal{C}, \mathcal{R})$ consisting of any two families

$$(15) \quad \mathcal{C} = \{\mathcal{C}_\iota\}_{\iota \in J} \quad \text{and} \quad \mathcal{R} = \{\mathcal{R}_\zeta\}_{\zeta \in M}$$

of connection and reflection maps.

An *excitation* is merely a distinguished process with values in the mesh boundary states. Let $B := \{\iota \mid \iota \in J \text{ and } \iota \text{ is not an interface}\}$ be defined as the *mesh boundary*, then an *excitation* is a process

$$(16) \quad \begin{aligned} e &: [0, T) \longrightarrow \prod_{\iota \in B} \mathcal{P}_\iota \\ t &\longmapsto e(t) = \pi^p \circ e(t) , \end{aligned}$$

i.e. e is a port process, and hence switches at entire multiples of the time step τ , and e generates *non-interface (mesh boundary)* states.

Definition 3. The *DSC process generated by $(\mathcal{C}, \mathcal{R})$ and excited by e* is the unique process $z(t) = (z^p, z^n)(t)$, which at every time $t \in [0, T)$ satisfies

$$(17) \quad \begin{aligned} z^p(t) &:= nb \circ z_{in}^n(t + \tau/2) + z_{out}^p(t) \\ z^n(t) &:= z_{in}^n(t) + nb \circ z_{out}^p(t + \tau/2) , \end{aligned}$$

the right-hand side being recursively defined through alternate iteration of

$$(18) \quad \begin{aligned} z_{in}^n(t + \tau/2) &:= nb \circ [\mathcal{C}[z_{out}^p](t) + e(t)] \\ z_{out}^p(t + \tau) &:= nb \circ \mathcal{R}[z_{in}^n](t + \tau/2) \end{aligned}$$

with, initially, $z_{in}^n(0) = z_{out}^p(0) = 0$.

In (18) \mathcal{C} and \mathcal{R} stand of course for application of all propagators \mathcal{C}_ι and \mathcal{R}_ζ of the families over the entire pertinent index sets (J and M). Remember also that nb denotes the node-boundary map (8).

It follows immediately that z^n and z_{in}^n thus defined are node processes, hence switch at odd integer multiples of $\tau/2$, while z^p , z_{out}^p are port processes (so they carry their superscripts aright).

Equations (17), (18) can still be simplified to

$$(19) \quad \begin{aligned} z^{p,n} &= z_{in}^{p,n} + z_{out}^{p,n} && \text{and} \\ z_{in}^p(t) &= \mathcal{C}[z_{out}^p](t) + e(t) \\ z_{out}^n(t + \tau/2) &= \mathcal{R}[z_{in}^n](t + \tau/2) , \end{aligned}$$

writing as usual z_{in}^p and z_{out}^n for

$$(20) \quad \begin{aligned} z_{in}^p(t) &:= nb \circ z_{in}^n(t + \tau/2) \\ nb \circ z_{out}^p(t) &=: z_{out}^n(t - \tau/2) . \end{aligned}$$

Comparing this to the TLM usage, one notes that in [14] port quantities z_{in}^p , z_{out}^p are first introduced. With these are then node quantities z_{in}^n , z_{out}^n identified (modulo the time shifts $\pm\tau/2$, just as in (18)) without yet explicitly mentioning the node-boundary isomorphism nb . We shall sometimes follow this usage and omit the symbol nb where this cannot lead to confusion.

So far, very few has been said about physical interpretations or any underlying dynamical equations. The characteristic structure of the DSC algorithm is in fact laid down with the given definitions. As will be seen in the next section, typical features and facts, many familiar from TLM, are derived with only the above requisites, as a more or less trivial exercise.

With respect to the dynamical *model equations* - which the algorithm has ultimately to solve and that determine the propagators \mathcal{R}_ζ , \mathcal{C}_ι , cf. section 4 - we reiterate the important general agreement that only *total fields* z^p , z^n , *not*, however, their *incident* and *outgoing components separately*, shall enter these equations. Accordingly, we admit only model equations between total fields. Quite generally, and modulo further restrictions (inferred in the next section), the DSC model equations should be of the types

$$(21) \quad \begin{aligned} \mathcal{F}^n[z_+^n][z^p] &\equiv 0 \\ \mathcal{F}^p[z_+^p][z^n] &\equiv 0 \quad , \end{aligned}$$

with causal functions \mathcal{F}^n , \mathcal{F}^p and shortly $[z_\pm] := [z](t \pm \tau/2)$. The $\tau/2$ time shifts in the arguments of either equations synchronize node and cell boundary switching in (21), such that the equations can be *strictly* solved, for *every* time $t \in [0, T)$ and are well-posed, in this sense. Of course, time shifts by $-\tau/2$ would also yield a synchronization. The resulting equations would, however, conflict with the causality property of \mathcal{R} and \mathcal{C} (and would require retarded propagators, instead).

Inspection of equations (21) shows that \mathcal{F}^n affects only the reflection cycle, while \mathcal{F}^p has impact only on the connection cycle. We are now dealing with the model equations in more detail.

4. THE DYNAMICAL MODEL EQUATIONS

The physical interpretation of a DSC system fixes, intuitively speaking, the terms in that states in \mathcal{P} are read as physical fields. More deliberately, certain states in \mathcal{P} are interpreted as distributional values (finite integrals, e.g.) of physical fields, which are localized in a mesh cell system.

Any interpretation requires, hence, in the first instance a geometric realization of the underlying regular mesh, wherein the relations between abstract cells, nodes, and boundary faces characterizing M are translated into relations between geometric objects, bounded subsets of \mathbb{R}^D , such as (in general) polyhedral mesh cells with their faces, e.g.

Given any geometric realization of M , a *physical interpretation* of a DSC system over M is, precisely, a family $I = \{I_\zeta^\iota\}_{\zeta \in M, \iota \in \partial\zeta}$ of continuous linear functions

$$(22) \quad I_\zeta^\iota : \mathcal{E}_\zeta^\iota \longrightarrow \mathcal{P}_\zeta \quad ,$$

each defined on a space \mathcal{E}_ζ^ι of smooth m -component vector fields in D -dimensional configuration space (i.e. $\mathcal{E}_\zeta^\iota \subset C^\infty(\mathbb{R}^D)^m$; $m \in \mathbb{N}$ depending on (ι, ζ)), such that I_ζ^ι has its distributional support on a cell face and its range in $\mathcal{P}_\zeta^p = \pi^p(\mathcal{P}_\zeta)$.

Note that index ι in (22) may optionally be read as a cell face label *or* as a multiindex referring to a set of ports on that cell face. Since we are dealing with vector-valued distributions (with range in \mathcal{P}) and the support

of every I_ζ^ι is required to be *localized on* a cell face (which can be weakened to at least *associated to* a face), there is essentially no difference in reading $z_{\iota,\zeta}^p = I_\zeta^\iota(Z)$ as a cell face state vector, or as an array of components (labelled by port indices) of such a vector. Thus, index ι in (22) may be thought of as implicitly labelling a subset of ports on face $\iota \in \partial\zeta$.

Attention is also drawn to the fact that the functions I_ζ^ι are *not* required to be *surjective* onto \mathcal{P}_ζ^p (i.e. not every state in \mathcal{P}_ζ^p must be directly related to a distribution in I). There is, for instance, no need to exclude from \mathcal{P}_ζ^p any functions or linear combinations of fields in *different* spaces \mathcal{E}^ι (which may represent a spatial finite difference of fields, as in the approximate gradient of the sample model in section 5).

The evaluation of nodal fields goes quasi pick-a-pack with I by applying the scattering channel concept of section 3.

Let s_ζ^ι denote the translational shift in \mathbb{R}^D from a node n_ζ into the (centre of the) face where I_ζ^ι has its support, cf. fig 1, and assume without loss of generality that $S_\zeta^\iota : Z(x) \mapsto Z(x + s_\zeta^\iota)$ is an inner map in \mathcal{E}_ζ^ι (otherwise take the closure of \mathcal{E}_ζ^ι under such transformations). Then clearly holds

Proposition 1. *For every $I_\zeta^\iota \in I$ there exists exactly one function $I_\zeta^{\iota\sim} : \mathcal{E}_\zeta^\iota \rightarrow \mathcal{P}_\zeta^n$ (note $I_\zeta^{\iota\sim} \notin I$), such that the following diagram is commutative*

$$(23) \quad \begin{array}{ccc} \mathcal{P}_\zeta^p & \xrightarrow{nb} & \mathcal{P}_\zeta^n \\ I_\zeta^\iota \uparrow & & \uparrow I_\zeta^{\iota\sim} \\ \mathcal{E}_\zeta^\iota & \xrightarrow{S_\zeta^\iota} & \mathcal{E}_\zeta^\iota \end{array}$$

$$i.e. \quad I_\zeta^{\iota\sim} \circ S_\zeta^\iota = nb \circ I_\zeta^\iota.$$

Proof. Mere retrospection of definitions. □

In the terminology of section 2 is $I_\zeta^{\iota\sim}$ the nodal image of the port(s) I_ζ^ι , and the pair of distributions $(I_\zeta^\iota, nb \circ I_\zeta^{\iota\sim})$ forms a scattering channel.

The dynamical DSC *model equations* are, in the line of the preceeding, to be read as finite difference equations *in time* between states $z = (z_{\iota,\zeta}^p, z_{\iota,\zeta}^n) \in \mathcal{P}$ that admit an interpretation as distributional values of physical fields $Z \in \mathcal{E}_\zeta^\iota$,

$$(24) \quad z_{\iota,\zeta}^p = I_\zeta^\iota(Z) \quad , \quad z_{\iota,\zeta}^n = I_\zeta^{\iota\sim}(Z) \quad .$$

Unlike classical FD equations between pointwise evaluated physical fields, the DSC model equations interrelate in many cases finite integrals over a line segment or face, e.g. - pointwise evaluation (with a Dirac measure as distribution) not excluded. The DSC approach is, in this respect, by far more versatile than the classical finite difference time domain method. So, the former permits, for instance, of generalizing to a non-orthogonal mesh Johns' TLM method [13] in much a simpler way, cf. [15], than the FDTD approach allows for Yee's method of approximation to Maxwell's equations [11].

A central principle underlying DSC schemes is *near-field interaction*. Like causality, this is already implicit in the (domains of) definition of the reflection and connection maps. Near-field interaction simply spells that only the fields in the immediate neighbourhood of a state z - precisely only those in \mathcal{P}_ζ if $z \in \mathcal{P}_\zeta^n$, and those in \mathcal{P}_ι if $z \in \mathcal{P}_\iota^p$, cf. (6, 9), along with their history, of course - determine the evolution of that state on the next updating step (note, this refers to fields evaluated in \mathcal{P} and not, for instance, to an exterior potential, which may still induce a time dependence of \mathcal{R} or \mathcal{C}).

In other words, an updated nodal state depends only on states of the pertinent cell, including its boundary, while the evolution of a port state is determined by states of the respective face and by nodal states of the adjacent cells.

It follows that the model equations (21) split into the two families

$$(25) \quad \mathcal{F}_\zeta^n[z_{\zeta+}^n][z_\zeta^p] \equiv 0, \quad z_\zeta \in \mathcal{P}_\zeta, \quad \zeta \in M$$

$$(26) \quad \mathcal{F}_\iota^p[z_{\iota+}^p][z_\iota^n] \equiv 0, \quad z_\iota \in \mathcal{P}_\iota, \quad \iota \in J.$$

(Remaining aware of the dependence upon ζ and ι of these equations, we can in general omit the subscripts, if there is no danger of confusion.)

Since the following analysis runs perfectly parallel for the dual equations, from now on it is confined to the implications of (25). - The reader may write down parallel statements for dual equations, at times, by exchanging port for nodal and incident for outgoing quantities, starting, for instance, with the cell boundary version (with \mathcal{C} in the place of \mathcal{R}) of the following:

Definition 4. Let $I = [0, T)$ be a *finite* interval (i.e. $T \in \mathbb{R}_+$). Then we shall say that \mathcal{R} *generates solutions* of the model equations (25) *on* I , if and only if for every sequence of incident nodal fields $[z_{in}^n]$ the (obviously unique) process $z = z_{in} + z_{out}$ that is recursively given by

$$(27) \quad \begin{aligned} z_{in}^p(t - \tau/2) &= nb \, z_{in}^n(t) \\ z_{out}^n(t) &= \mathcal{R}[z_{in}^n](t) \\ z_{out}^p(t + \tau/2) &= nb \, z_{out}^n(t), \end{aligned}$$

algebraically solves equations (25) (identically on I). Sometimes, we are then simply saying that \mathcal{R} *solves* the model equations *on that (finite !) interval*.

Remark.

- (i) Note that Definition 4 refers to a purely *algebraic property* of \mathcal{R} that is not yet related to any questions of stability, for instance (cf. also the Remark to Theorem 1).
- (ii) If \mathcal{R} solves equations (25) on I , then in particular every process generated by $(\mathcal{C}, \mathcal{R})$ in the sense of Definition 4 solves (25) on I , since every such process obviously satisfies (27) (cf. (20)).

The least awkward (fortunately frequently encountered) situation is brought about with homogeneous linear equations, i.e. for the evolution of nodal states

$$(28) \quad \mathcal{F}^n[z_+^n][z^p] = \sum_{\mu=0}^{\infty} \phi_\mu z^n(t + \tau/2 - \mu\tau) + \psi_\mu z^p(t - \mu\tau) \equiv 0,$$

with linear and possibly time dependent operators

$$\phi_\mu : \mathcal{P}^n \rightarrow \mathcal{J} \quad , \quad \psi_\mu : \mathcal{P}^p \rightarrow \mathcal{J}$$

into any linear space \mathcal{J} wherein \mathcal{F} has its range. Similar dual equations $\mathcal{F}^p[z_+^p][z^n] \equiv 0$ determine the linear evolution of the port states during the connection cycle.

Many, if not almost all (viz. all but a finite number) of the ϕ_μ, ψ_μ may be zero. Any maximum $\mu \in \mathbb{N} \cup \{\infty\}$, such that $\phi_\mu \neq 0$ or $\psi_\mu \neq 0$, is called the (*dynamical*) *order* of the model equations (and in general equals the order in time of the integro-differential equations which physically describe the underlying dynamical problem in terms of smooth fields).

The following statement provides a theoretical means for computing the reflection map of equation (28) recursively.

Theorem 1. *Let $\phi_0 : \mathcal{P}^n \rightarrow \mathcal{J}$ be bijective (i.e. one-to-one and onto). Then \mathcal{R} solves equation (28) on a finite interval $[0, T)$, if and only if for every $t \in [0, T)$*

$$\begin{aligned} \mathcal{R}[z_{in}^n](t) &= z_{out}^n(t) = \\ &= (-\phi_0)^{-1} \sum_{\mu=0}^{\infty} \{ (\phi_\mu + \psi_\mu nb) z_{in}^n(t - \mu\tau) + \\ &\quad + (\phi_{\mu+1} + \psi_\mu nb) z_{out}^n(t - \tau - \mu\tau) \} . \end{aligned}$$

Proof. Substituting in (28) for $z^{p,n}$ the right-hand sides of (17) and using equations (20) yields for $t < T$ on a time domain trivially extended over the negative axis

$$\begin{aligned} \sum_{\mu=0}^{\infty} \{ \phi_\mu [z_{in}^n(t + \tau/2 - \mu\tau) + z_{out}^n(t + \tau/2 - \mu\tau)] + \\ + \psi_\mu nb [z_{in}^n(t + \tau/2 - \mu\tau) + z_{out}^n(t - \tau/2 - \mu\tau)] \} \equiv 0 , \end{aligned}$$

which for invertible ϕ_0 and $t' := t + \tau/2$ is equivalent to the recursion formula of the theorem. \square

Remark. For every $t < T < \infty$ the sum in Theorem 1 is actually finite, hence convergence is not a question, as long as one abstains from considering limits. For finite T the theorem conveys *purely algebraic relations* inherited from the *structure of the DSC process*, as outlined in section 3, (17, 18). Questions of convergence and stability that appear for $T \rightarrow \infty$ are still being treated.

If ϕ_0 is *not* bijective, then the model equations (28) are incomplete in that they do not determine a well-defined and unique reflection propagator (in each cell). We shall therefore require that the *uniqueness condition*

$$(U) \quad \phi_0 : \mathcal{P}^n \rightarrow \mathcal{J} \text{ is bijective} \quad (\text{i.e. a linear isomorphism})$$

shall always be satisfied. Clearly, (28) then defines an explicit scheme.

The model equations of the classical TLM method discretize Maxwell's equations. So, they are linear and first order in time, viz. of the type

$$(29) \quad \phi_0 z^n(t + \tau/2) + \phi_1 z^n(t - \tau/2) + \psi_0 z^p(t) ,$$

with time independent operators $\phi_{0,1}$ and ψ_0 , which are derived in [19, 15], for instance. Of the same type are the discretized diffusion equations. Theorem 1 applied to this special situation yields

Corollary 1. *The (for given time step unique) reflection map that solves on a finite interval the first order linear equations (29) with time independent $\phi_{0,1}$ and ψ_0 is*

$$(30) \quad \begin{aligned} \mathcal{R}[z_{in}^n](t) &= z_{out}^n(t) = \\ &= K z_{in}^n(t) + L \sum_{\nu=1}^{\infty} N^{\nu-1} M z_{in}^n(t - \nu\tau), \end{aligned}$$

wherein

$$\begin{aligned} K &= -Id - \phi_0^{-1} \psi_0 n b \\ L &= -\phi_0^{-1} \\ M &= +\phi_1 + (\phi_1 + \psi_0 n b) \underbrace{(-\phi_0^{-1})(\phi_0 + \psi_0 n b)}_K \\ N &= -(\phi_1 + \psi_0 n b) \phi_0^{-1}. \end{aligned}$$

Proof. By induction, applying Theorem 1 to an incident Dirac pulse

$$z_{in}^n(t) := \mathbf{z} \chi_{[0, \tau)}(\mathbf{t} - \tau/2)$$

with any fixed state vector $\mathbf{z} \in \mathcal{P}^n$; χ_I denotes the characteristic function of interval I (which equals 1 for every argument in I and 0 elsewhere). By linearity the statement then holds for arbitrary incident processes $z_{in}^n(t)$, each of them being writable as a superposition of Dirac processes that start at subsequent time steps. \square

Remark. A sufficient condition for convergence of the propagator series (30) (applied to any finite incident pulse z_{in}^n) in the limit $t \rightarrow \infty$ is obviously

$$(31) \quad \|N\|_H < 1, \quad$$

wherein

$$(32) \quad \|N\|_H := \max \{ |\lambda|; \lambda \text{ eigenvalue of } N \}$$

denotes the Hilbert (spectral) norm of N . In fact, that condition is sufficient for algorithm stability of the Maxwell field TLM model, as shown in [19, 15]. Any first order linear process is clearly stable, if the Hilbert norms of K, L, M, N are bounded by 1 (strictly for K and N), since the propagator \mathcal{R} is *contractive* then. In general this can be ensured with bounds for the time step (if necessary, in combination with a transformation (34)).

For linear model equations of *any* finite order, recursion formulae that generalize (30) are easily derived from Theorem 1, e.g. [14], equation (32).

Corollary 2. *With K, L, M, N as above, the DSC process solving (29) admits a representation as a 'deflected' scattering process*

$$(33) \quad \begin{pmatrix} z_{out}^n(t) \\ d(t) \end{pmatrix} = \begin{pmatrix} K & L \\ M & N \end{pmatrix} \begin{pmatrix} z_{in}^n(t) \\ d(t - \mu\tau) \end{pmatrix},$$

the deflection $d(t)$ being recursively completely defined with the universally admitted initial conditions $d|_{t < 0} = 0$.

Proof. Immediate consequence of Corollary 1 \square

Remark. Note that there remains an arbitrariness in the definition of the operators L , M , and N in Corollaries 1, 2. In fact, any invertible transformation $I : \mathcal{J} \rightarrow \mathcal{J}$ together with the simultaneous replacements of L , M , and N by, respectively,

$$(34) \quad L^\sim := L \circ I^{-1}, \quad M^\sim := I \circ M, \quad \text{and} \quad N^\sim := I \circ N \circ I^{-1}$$

clearly do not alter the propagator \mathcal{R} , i.e. generates the same DSC process.

The corollaries offer solutions of first order linear equations with time independent operator coefficients which are complete in the sense of (U). They thus cover the entire field of classical TLM (with connection maps that are trivial in reducing essentially to identity).

In certain situations it may be useful, or necessary, to integrate some new (possibly non-linear) interactions into a given DSC model. Sometimes, this can be carried out by adding suitable coupling terms to the equations of the yet existing model. We therefore consider *perturbed* model equations of the type

$$(35) \quad \mathcal{F}^\sim[z_+^n][z^p] \equiv \mathcal{F}^n[z_+^n][z^p] + \mathcal{J}[z_-^n][z^p] \equiv 0$$

(here exemplary for nodal perturbations), wherein \mathcal{J} denotes any causal map into \mathcal{J} . The $(-\tau/2)$ time shift in the first argument of \mathcal{J} again synchronizes port and node switching. Note that the time shift is negative, here. This is to ensure that the perturbation \mathcal{J} cannot destroy the uniqueness conditions (U) in the case of a *linear* function \mathcal{F}^n , and to preserve explicitness of the updating relations, in general. The importance of this condition becomes clear in the proof of the following formula.

Proposition 2 (Deflection Formula). *Let the reflection map \mathcal{R} generate solutions of the linear equations (28) on a finite interval $I = [0, T)$. Then \mathcal{R}^\sim solves the perturbed equations (35) on I , if and only if the so-called deflection*

$$\mathcal{D} := \mathcal{R}^\sim - \mathcal{R}$$

satisfies recursively

$$\begin{aligned} \phi_{0|t} \mathcal{D}_{|t+\tau/2} &= - \mathcal{J}[z_-^n][z^p]_{|t} \\ &- \sum_{\mu \in \mathbb{N}} (\phi_{\mu+1|t} + \psi_{\mu|t} nb) \mathcal{D}_{|t-\tau/2-\mu\tau} \quad . \end{aligned}$$

Proof. Under the given assumptions \mathcal{R}^\sim solves equations (35) on I , if and only if for every incident sequence $[z_{in}^n]$, and short-hand

$$\begin{aligned} w_{out}^n &:= \mathcal{R}[z_{in}^n], & w &:= z_{in} + w_{out} \\ z_{out}^n &:= \mathcal{R}^\sim[z_{in}^n], & z &:= z_{in} + z_{out} \quad , \end{aligned}$$

i.e. $\mathcal{D} = z_{out}^n - w_{out}^n = \mathcal{R}^\sim - \mathcal{R}$, the following is true

$$\begin{aligned} \mathcal{F}^\sim[z_+^n][z^p] &= \\ &= \mathcal{F}^n[z_+^n][z^p] + \mathcal{J}[z_-^n][z^p] = 0 \quad . \end{aligned}$$

Using (28), the last line reads

$$\begin{aligned}
 -\mathcal{J}[z_-^n][z^p]_t &= \\
 &= \sum_{\mu \in \mathbb{N}} \left\{ \phi_{\mu|t} (z_{in|t+\tau/2-\mu\tau}^n + \underbrace{w_{out|t+\tau/2-\mu\tau}^n + \mathcal{D}_{|t+\tau/2-\mu\tau}}_{z_{out|t+\tau/2-\mu\tau}^n}) + \right. \\
 &\quad \left. + \psi_{\mu|t} nb (z_{in|t+\tau/2-\mu\tau}^n + \underbrace{w_{out|t-\tau/2-\mu\tau}^n + \mathcal{D}_{|t-\tau/2-\mu\tau}}_{z_{out|t-\tau/2-\mu\tau}^n}) \right\}.
 \end{aligned}$$

In virtue of the linearity of the ϕ_μ , ψ_μ , the latter identity holds iff

$$\begin{aligned}
 -\mathcal{J}[z_-^n][z^p]_t &= \underbrace{\mathcal{F}^n[w_+^n][w^p]}_{\mathbf{0} \text{ by (28)}} + \\
 &+ \phi_{0|t} \mathcal{D}_{|t+\tau/2} + \sum_{\mu \in \mathbb{N}} (\phi_{\mu+1|t} + \psi_{\mu|t} nb) \mathcal{D}_{|t-\tau/2-\mu\tau},
 \end{aligned}$$

which is the recurrence relations of the Proposition 2. \square

Corollary (Deflected processes). *Let \mathcal{R} solve (28) on a finite interval I and $\phi_0 : \mathcal{P} \rightarrow \mathcal{I}$ be any bijective operator (that thus satisfies the completeness conditions (U)). Then*

$$\mathcal{D}_{|t+\tau/2} := -\phi_{0|t}^{-1} \left\{ \mathcal{J}[z_-^n][z^p]_t + \sum_{\mu \in \mathbb{N}} (\phi_{\mu+1|t} + \psi_{\mu|t}) \mathcal{D}_{|t-\tau/2-\mu\tau} \right\}$$

with initial conditions $\mathcal{D}_{|t<0} \equiv 0$ defines recursively a causal operator \mathcal{D} , such that $\mathcal{R}^\sim := \mathcal{R} + \mathcal{D}$ solves equations (35) on I .

Concluding this section, we stress once again that Theorem 1 and the following propositions and corollaries apply just as well to the connection cycle, i.e. cell interface scattering, provided the replacements (25) by (26), \mathcal{R} by \mathcal{C} , \mathcal{P}_ζ by \mathcal{P}_ι , port by node superscripts, and incoming by outgoing fields (and vice-versa) are simultaneously made. - Note, however, that any *excitations may temporarily violate* the model equations at a *mesh boundary* face. The model developer is encouraged to care for physically appropriate excitations.

5. A NON-ORTHOGONAL HEAT PROPAGATION [DIFFUSION] SCHEME

The physical interpretation underlying the following application relates a smoothly varying (viz. in time and space continuously differentiable, C^1 -) temperature field T , evaluated as T^p at the face centre points and as T^n in the nodes of a of non-orthogonal hexahedral mesh, to total states $z_\mu^{p,n}$ of a DSC model. In this section, we confine ourselves to derive the model equations for the connection and reflection cycles of a DSC heat propagation (diffusion) scheme. Since the equations are linear and of dynamical order 0 and 1, respectively - as will be seen - they can be processed, following the guidelines of the last section. In the end, we display some computational results of a dispersion test carried out with this model.

In order to simplify the notation, we follow Einstein's convention to sum up over identical right-hand (!) sub and superscripts within all terms where such are present (summation is not carried out over any index that also appears somewhere at the left-hand side of a pertinent symbol - thus, in $(-1)^\kappa a_\kappa^\lambda b_\lambda c$ the sum is made over λ but not over κ).

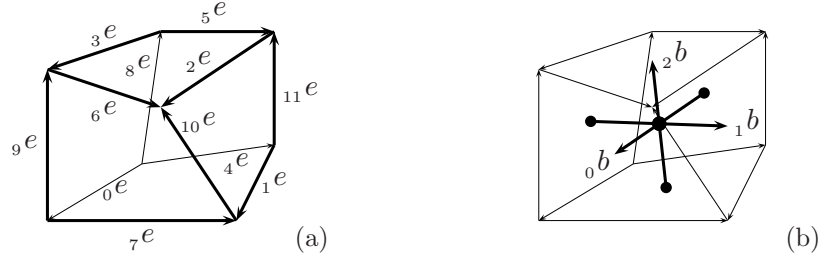


FIGURE 2. *Non-orthogonal hexahedral mesh cell.*
 (a) *Edge vectors.* (b) *Node vectors.*

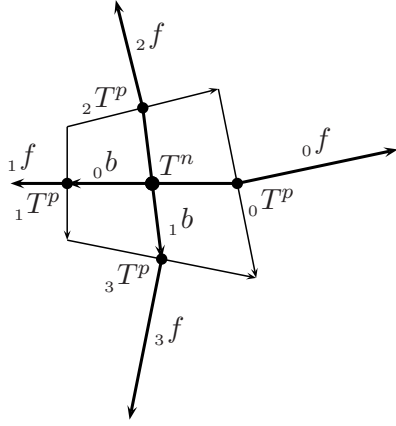


FIGURE 3. *Face vectors and temperature points (nodal section).*

The shape of a hexahedral cell is completely determined by its 12 *edge vectors* $(_\nu e)_{\nu=0,\dots,11}$ (a cell index being omitted). Also, with the labelling scheme of fig 2a, *node vectors* $(_\mu b)_{\mu=0,1,2}$ and *face vectors* $(_\iota f)_{\iota=0,\dots,5}$ are defined as

$(edge vector indices cyclic modulo 12, and \wedge denoting the wedge ('cross') product in \mathbb{R}^3).$

At every face $\iota \in \{0, \dots, 5\}$ of a mesh cell, and for any given $\tau \in \mathbb{R}_+$, the following time shifted finite temperature differences in directions $_\mu b$ ($\mu = 0, 1, 2$) form the vector valued function

$$(37) \quad \iota \nabla^B T_\mu(t, \tau) := \begin{cases} 2(-1)^\iota (T^n|_{t-\tau/2} - \iota T^p|_t) & \text{if } \mu = [\iota/2] \\ (_{2\mu+1} T^p - _{2\mu} T^p)|_{t-\tau} & \text{if } \mu \neq [\iota/2] \end{cases}$$

($[x]$ denotes the integer part of $x \in \mathbb{R}$). The time increments are chosen to attain technical consistence with the updating conventions of DSC schemes. They do not destroy convergence, as easily seen: In fact, in the centre point of face ι the vector ${}_{\iota}\nabla^B T$ approximates in the first order of the time increment τ , and of the linear cell extension, the scalar products of the node vectors with the temperature gradient ∇T . Let, precisely, for $\epsilon \in \mathbb{R}_+$ the ϵ -scaled cell be that one with edge vectors ${}_{\iota}e^{\sim} := \epsilon {}_{\iota}e$ and with the centre point on face ι held fixed. Let also ${}_{\iota}\nabla^{B\sim} T_{\mu}$ denote function (37) for the scaled cell (with node vectors ${}_{\mu}b^{\sim} = \epsilon {}_{\mu}b$). Then at the fixed point holds

$$(38) \quad \langle {}_{\mu}b, \text{grad}(T) \rangle = {}_{\mu}b \cdot \nabla T = \lim_{\epsilon \rightarrow 0} \lim_{\tau \rightarrow 0} \frac{1}{\epsilon} {}_{\iota}\nabla^{B\sim} T_{\mu},$$

as immediately follows from the required C^1 -smoothness of the temperature field T .

To recover, in the same sense and order of approximation, the gradient ∇T from (37), observe that for every orthonormal basis $({}_{\nu}u)_{\nu=0,\dots,m-1}$ of $V = \mathbb{R}^m$ or \mathbb{C}^m , and for an arbitrary basis $({}_{\mu}b)_{\mu=0,\dots,m-1}$ with coordinate matrix $\beta_{\nu}^{\mu} = \langle {}_{\nu}u, {}_{\mu}b \rangle$, the scalar products of any vector $a \in V$ with ${}_{\mu}b$ are

$$(39) \quad \underbrace{\langle {}_{\mu}b, a \rangle}_{=: \alpha_{\mu}^B} = \sum_{\nu=0}^{m-1} \underbrace{\langle {}_{\mu}b, {}_{\nu}u \rangle}_{(\bar{\beta}_{\mu}^{\nu}) = (\beta_{\nu}^{\mu})^*} \underbrace{\langle {}_{\nu}u, a \rangle}_{=: \alpha_{\nu}} = \bar{\beta}_{\mu}^{\nu} \alpha_{\nu}.$$

(At the right-hand side, and henceforth, we follow Einstein's convention to sum up over identical sub and superscripts within terms, where such are present). It follows that

$$(40) \quad \alpha_{\nu} = \gamma_{\nu}^{\mu} \alpha_{\mu}^B, \quad \text{with} \quad (\gamma_{\nu}^{\mu}) := ((\beta_{\nu}^{\mu})^*)^{-1}.$$

Loosely speaking, the scalar products of any vector with the basis vectors ${}_{\mu}b$ transform into the coordinates of that vector with respect to an orthonormal basis ${}_{\nu}u$ via multiplication by matrix $\gamma = (\beta^*)^{-1}$, where $\beta_{\nu}^{\mu} = \langle {}_{\nu}u, {}_{\mu}b \rangle$, i.e. β is the matrix of the coordinate (column) vectors ${}_{\mu}b$ with respect to the given ON-basis ${}_{\nu}u$, and γ is the adjoint inverse of β .

This applied to the node vector basis ${}_{\mu}b$ and (38) yields the approximate temperature gradient at face ι as

$$(41) \quad {}_{\iota}\nabla T_{\nu} = \gamma_{\nu}^{\mu} {}_{\iota}\nabla^B T_{\mu}.$$

Thus, the heat current *into* the cell through face ι with face vector components ${}_{\iota}f^{\nu} = \langle {}_{\iota}f, {}_{\nu}u \rangle$, $\nu \in \{0, 1, 2\}$, is

$$(42) \quad {}_{\iota}J = \lambda_H {}_{\iota}f \cdot {}_{\iota}\nabla T = \underbrace{\lambda_H {}_{\iota}f^{\nu} \gamma_{\nu}^{\mu}}_{=: {}_{\iota}s^{\mu}} {}_{\iota}\nabla^B T_{\mu} = {}_{\iota}s^{\mu} {}_{\iota}\nabla^B T_{\mu},$$

λ_H denoting the heat conductivity in the cell.

The heat current through every interface is conserved, i.e. between any two adjacent cells ζ, χ with common face, labelled ι in cell ζ and κ in χ , applies

$$(43) \quad {}_{\iota}^{\zeta}J = - {}_{\kappa}^{\chi}J.$$

Also, the nodal temperature change in cell ζ is

$$(44) \quad \frac{dT^n}{dt} = \frac{1}{c_v V} (S + \sum_{\iota=0}^5 {}_{\iota}J),$$

where c_v denotes the heat capacity (per volume), V the cell volume, and S any heat source(s) in the cell.

We finally introduce quantities ${}_{\iota}z_{\mu}^{p,n}$ ($\iota = 0, \dots, 5$; $\mu = 0, 1, 2$), which still smoothly vary in time with the temperature T (and that are hence not yet DSC states, but will later be updated as such)

$$(45) \quad {}_{\iota}z_{\mu}^n(t) := \begin{cases} 2(-1)^{\iota} T^n|_t & \text{if } \mu = [\iota/2] \\ ({}_{2\mu+1}T^p - {}_{2\mu}T^p)|_{t-\tau/2} & \text{else} \end{cases}$$

and

$$(46) \quad {}_{\iota}z_{\mu}^p(t) := \begin{cases} 2(-1)^{\iota} {}_{\iota}T^p|_t & \text{if } \mu = [\iota/2] \\ {}_{\iota}z_{\mu}^n(t - \tau/2) & \text{else.} \end{cases}$$

From (37, 42) follows

$$(47) \quad \begin{aligned} {}_{\iota}J|_{t+\tau/2} &= {}_{\iota}S^{\mu} ({}_{\iota}z_{\mu}^n|_t - 2(-1)^{\iota} \delta_{\mu}^{[\iota/2]} {}_{\iota}T^p|_{t+\tau/2}) \\ &= {}_{\iota}S^{\mu} ({}_{\iota}z_{\mu}^n|_t - \delta_{\mu}^{[\iota/2]} {}_{\iota}z_{\mu}^p|_{t+\tau/2}) \quad . \end{aligned}$$

This, with (43) and continuity of the temperature at the interface, ${}_{\zeta}T^p = {}_{\kappa}^x T^p$, together with (46) imply

$$(48) \quad {}_{\zeta}z_{\mu}^p|_{t+\tau/2} = \begin{cases} \frac{{}_{\zeta}S^{\mu} {}_{\zeta}z_{\mu}^n|_t + {}_{\kappa}^x S^{\nu} {}_{\kappa}^x z_{\nu}^n|_t}{{}_{\zeta}S^{[\iota/2]} + (-1)^{\iota+\kappa} {}_{\kappa}^x S^{[\kappa/2]}} & \text{if } \mu = [\iota/2] \\ {}_{\zeta}z_{\mu}^n|_t & \text{else,} \end{cases}$$

which form a complete set of recurrence relations for z^p (given z^n) and so can be taken as model equations for the connection cycle of a DSC algorithm.

Equations (44), discretely integrated in time the balanced form with increment τ , yield

$$(49) \quad T^n|_{t+\tau/2} = T^n|_{t-\tau/2} + \frac{\tau}{c_v V} (S + \sum_{\iota=0}^5 {}_{\iota}J|_t),$$

i.e., with (45, 46, 47), the recurrence relations

$$(50) \quad {}_{\iota}z_{\mu}^n|_{t+\tau/2} = \begin{cases} {}_{\iota}z_{[\iota/2]}^n|_{t-\tau/2} + \frac{(-1)^{\iota}\tau}{2c_v V} \{ S + \\ + \sum_{\iota=0}^5 {}_{\iota}S^{\nu} ({}_{\iota}z_{\nu}^n|_{t-\tau/2} - \delta_{\nu}^{[\iota/2]} {}_{\iota}z_{\nu}^p|_t) \} & \text{if } \mu = [\iota/2] \\ -\frac{1}{2} ({}_{2\mu+1}z_{\mu}^p + {}_{2\mu}z_{\mu}^p)|_t & \text{else,} \end{cases}$$

which provide a complete set of model equations for the reflection cycle of a DSC algorithm. Note that the first line, modulo the factor $2(-1)^{\iota}$, updates the nodal temperature - which, of course, has to be carried out only once per iteration cycle, if the total states are directly updated. In this special example (and many others) the 'squared' DSC state space concept, cf. (6), creates a redundancy needed by the Johns cycle due to (18) in Definition 3.

Equations (48, 50) may be directly taken as updating relations for total quantities of a DSC scheme, and they can be further processed for deriving the reflection and connection maps, and stability bounds for the time

step. The proceeding is canonical and amounts in essence to a straightforward transcription of the model equations along the lines of Theorem 1 and corollaries.

It is particularly easy to couple this heat conduction model within one and the same mesh to a Maxwell field TLM model in the non-orthogonal setting [15]. In fact, with the node vector definition in [16], the total node voltages are just the scalar products of ${}_{\mu}b$ with the electric field, hence the dielectric losses and heat sources per cell become

$$(51) \quad S = \frac{1}{2} \sigma V E^{\nu} \overline{E_{\nu}} = \frac{1}{2} \sigma V \sum_{\nu} |\gamma_{\nu}^{\mu} U_{\mu}^n|^2 ,$$

for a frequency domain (complex) TLM algorithm, cf. [14] ; $\sigma = 2\pi f \epsilon \tan(\delta)$ denotes the effective loss current conductivity at frequency f in a mesh cell of absolute permittivity ϵ and dielectric loss factor $\tan(\delta)$, $\gamma = (\beta^*)^{-1}$, as in (40). In SPINNERS's implementation, the model couples also to magnetic and skin effect losses.

Fig 4 finally displays the computed results of a dispersion test, using a square mesh with non-orthogonal cells. It turns out that the heat conduction properties of the mesh are highly insensitive to cell shape and orientation (as of course should be the case).

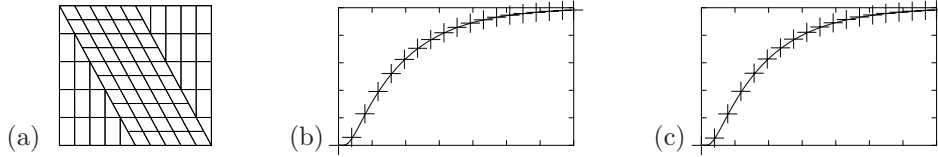


FIGURE 4. Transverse heat conduction over a square mesh using non-orthogonal cells. A Heaviside temperature step is imposed on one side and the transient temperature computed at the opposite side, assuming adiabatic boundary conditions on all but the heated sides.

DSC results (+) are plotted over analytical solution (curve).

(a) The mesh. (b) Horizontal (c) vertical propagation.

6. CONCLUSIONS

This paper dealt with prospective extensions of the Transmission Line Matrix method along Johns' line which allow to overcome certain of its limitations, connected with the transmission line concept. As has been technically demonstrated, the TLM method should be generalized in two major directions, by replacing transmission line links between cells with scattering channels in terms of paired distributions, and in admitting non-trivial connections at cell interfaces. This leads to a novel class of dual scattering

channel schemes which offer enlarged modeling potentiality - and a wide field of future research.

REFERENCES

- [1] Rebel, J.N., On the Foundations of the Transmission Line Matrix Method, Thesis, TU München, 2000
- [2] Johns, P.B. and Beurle, R.L. Numerical solution of 2-dimensional scattering problems using transmission line matrix, Proc. IEEE, 118, pp. 1203-1208, 1971
- [3] Proceedings of the 1st Int. Workshop on Transmission Line Matrix (TLM) Modelling, Victoria, 1995
- [4] Proceedings of the 2nd Int. Workshop on Transmission Line Matrix (TLM) Modelling, TU München, 1997
- [5] Proceedings of the 3rd Int. Workshop on Transmission Line Matrix (TLM) Modelling, Nice, 1999
- [6] Christopoulos, C., *The Transmission-Line Modeling Method TLM*, IEEE Press, New York 1995
- [7] De Cogan, D., *Transmission Line Matrix (TLM) Techniques for Diffusion Applications*, Gordon and Breach, 1998
- [8] Trenkic, V., The TLM Method with Advanced Condensed Nodes, Proceedings of the 2nd Int. Workshop on Transmission Line Matrix (TLM) Modelling, TU München, 1997
- [9] Chen, Z., Ney, M.M., Hoefer, W.J.R, A New Finite-Difference Formulation and its Equivalence with the TLM Symmetrical Condensed Node, IEEE Trans. Microwave Theory Tech., vol. 39, pp. 2160-2169, December 1991
- [10] Akhtarzad, S., Johns, P.B., Solution of 6-components electromagnetic fields in three dimensions and time by the T.L.M. method, Electron. Lett. vol. 10, pp. 535-537, Dec. 12, 1974
- [11] Yee, K.S., Numerical Solution of Initial Boundary Value Problems Invoking Maxwell's Equations in Isotropic Media, IEEE Trans. Antennas and Propagation, 14 (3), pp 302-307, May 1966
- [12] Kunz, K.S., Luebbers, R.J., *The Finite Difference Time Domain Method for Electromagnetics*, CRC Press, 1993
- [13] Johns, P.B., A symmetrical Condensed Node for the TLM Method, IEEE Trans. Microwave Theory Tech., vol. 35, pp. 370-377, April 1987
- [14] Hein, S., Gauge techniques in time and frequency domaine TLM, Computer Physics Communications, pp. 77-89, 2001
- [15] Hein, S., Finite-difference time-domain approximation of Maxwell's equations with nonorthogonal condensed TLM mesh, Int. J. Num. Modelling, pp. 179-188, 1994
- [16] Hein, S., Synthesis of TLM Algorithms in the Propagator Integral Framework, Proceedings of the 2nd. Int. Workshop on Transmission Line Matrix Modeling (TLM) - Theory and Applications, pp. 1-11, Munich, October 1997
- [17] Hein, S., TLM numerical solution of Bloch's equations for magnetized gyrotropic media, Appl. Math. Modelling, pp. 221-229, 1997
- [18] Hein, S., A TLM node for superconducting boundary illustrating the propagator approach, Spinner Report E017, München 1992
- [19] Hein, S., Consistent finite difference modelling of Maxwell's equations with lossy symmetrical condensed TLM node, Int. J. Num. Modelling, pp. 207-220, 1993
- [20] Hoefer, W. J. R., The Transmissionline Matrix (TLM) Method, in Numerical Techniques for Microwave and Millimeter-Wave Passive Structures, T. Itoh ed. John Wiley & Sons, 1989

SPINNER RF LAB, AIBLINGER STR.30, D-83620 WESTERHAM, GERMANY

E-mail address: s.hein@spinner.de